STUDY OF RESISTIVE-WALL BEAM BREAKUP

N. Nakamura
ISSP, University of Tokyo, 5-1-5 Kashiwanoha, Kashiwa, Chiba 277-8581, Japan

Abstract

Beam breakup (BBU) caused by the long-range transverse resistive-wall wake in ERLs is studied mainly with a developed simulation program. The simulation program is useful and essential for understanding the resistive-wall BBU behaviours especially in the parameter ranges and initial conditions where the asymptotic expressions analytically derived are invalid. The simulation results show that the position displacement or orbit distortion due to the wake increase in proportion to the square root of the time and the wake strength in the early stage of the resistive-wall BBU and that, in the case of the test ERL in Japan, the maximum position displacements reach 3% and 1% of the initial position offset with all the quadrupole magnets off and on at 77 μs. Effects of a small-gap insertion device (ID) duct and ID focusing are also investigated.

INTRODUCTION

In storage rings such as synchrotron light sources, transverse coupled-bunch instabilities due to long-range resistive-wall wake as well as other instabilities due to RF cavities and ion trapping are sometimes observed against radiation damping [1]. It is expected that transverse multi-bunch resistive-wall beam breakup can be a serious problem in high-current ERLs. While the BBU due to HOMs of superconducting cavities has been much investigated, the resistive-wall beam breakup (RWBBU) has been hardly studied and only the asymptotic expressions were analytically derived in simple and limited conditions [2]. In this paper, more detailed study of the RWBBU with a simulation program is presented.

RESISTIVE-WALL WAKE

The long-range transverse resistive-wall wake-function for a round pipe with a radius b, length L and electrical conductivity σ_c is expressed by

$$W_\perp = -\frac{cL}{\pi b^3 z^{1/2}}\sqrt{\frac{Z_0}{\pi\sigma_c}}, \tag{1}$$

where c, Z_0 and z are the velocity of light, the vacuum impedance and the distance from the wake source such as a preceding bunch. Eq. (1) is valid under the following condition:

$$\sqrt[3]{\frac{b^2}{\sigma_c Z_0}} << z << b^2\sigma_c Z_0 \tag{2}$$

An electron is kicked by such wake and the transverse kick by a preceding bunch with the position y and the distance z is given by

$$\Delta\theta_y = -\frac{e^2N}{E}W_\perp \cdot y = \frac{e^2N}{E}\cdot\frac{cL}{\pi b^3 z^{1/2}}\sqrt{\frac{Z_0}{\pi\sigma_c}}\cdot y, \tag{3}$$

where E is the beam energy and N is the electron number in the bunch. The wake-field is easily cumulated in the multi-bunch beam, because it is slowly decayed following Eq. (1). It also depends on pipe characteristics such as pipe radius, electrical conductivity and length. On the other hand, the long-range longitudinal wake-function is given by

$$W_{//} = -\frac{cL}{\pi b z^{3/2}}\sqrt{\frac{Z_0}{\pi\sigma_c}}, \tag{4}$$

In this case, cumulation of the resistive-wall wake-field is relatively smaller than in the transverse case. Thus only the transverse beam breakup is treated here.

ASYMPTOTIC EXPRESSION

Here the asymptotic expressions [2] for the RWBBU are reviewed. The asymptotic expressions were analytically derived from the following equation:

$$y_M''(s) + k_y^2 y_M(s) = \sum_{N=1}^{M-1}\frac{a}{\sqrt{M-N}}y_N(s) \quad (M \ge 2) \tag{5}$$

$$a \equiv \frac{e^2N}{E}\cdot\frac{c}{\pi b^3(c\tau_B)^{1/2}}\sqrt{\frac{Z_0}{\pi\sigma_c}} = \frac{eI_B}{E}\cdot\frac{(c\tau_B)^{1/2}}{\pi b^3}\sqrt{\frac{Z_0}{\pi\sigma_c}}$$

where τ_B and k_y are bunch time separation and external focusing strength, and I_B is the average beam current defined by eN/τ_B. Eq. (5) shows equation of motion for the M-th bunch ($M \ge 2$) for the case where an electron beam consisting of a series of identical point-like bunches passes through a round pipe with uniform external focusing. For two extreme cases, no focusing (NF) case and strong focusing (SF) case, the asymptotic expressions are given by

$$y_M(s) = \frac{y_{00}}{\sqrt{2\pi}}\left(\frac{t_{NF}}{t}\right)^{\frac{1}{10}}\cdot exp\left[\left(\frac{t}{t_{NF}}\right)^{\frac{1}{5}}\right] \tag{6}$$

$$t_{NF} \equiv \frac{\tau_B}{4\pi}\left(\frac{4}{5}\right)^5\frac{1}{a^2s^4} \tag{7}$$

and

$$y_M(s) = \frac{y_{00}}{\sqrt{2\pi}}\left(\frac{t_{SF}}{t}\right)^{\frac{1}{6}}exp\left[\left(\frac{t}{t_{SF}}\right)^{\frac{1}{3}}\right]cos\left[\sqrt{3}\left(\frac{t}{t_{SF}}\right)^{\frac{1}{3}} - k_y s - \frac{\pi}{6}\right] \tag{8}$$

$$t_{SF} \equiv \frac{16k_y^2\tau_B}{\pi}\left(\frac{2}{3}\right)^3\frac{1}{a^2s^2} \tag{9}$$

respectively. The initial condition is that all the bunches have the same position offset $y_M(0)=\ldots y_2(0)=y_1(0)\equiv y_{00}$ at the pipe entrance and the time t from the injection of the initial bunch is approximately equal to $M\tau_B$ for infinite bunch number ($M\to\infty$). The t_{NF} and t_{SF} are the growth times for the two cases.

These expressions require some conditions to be valid. These conditions are as follows:
(i) NF case

$$\alpha_1^{4/5} << 1, \quad \frac{a\sqrt{\pi}}{k_y^2 \alpha_1^{2/5}} >> 1, \quad t >> \frac{s}{c}, \quad t >> t_{NF} \tag{10}$$

(ii) SF case

$$\alpha_2^{2/3} << 1, \quad \frac{k_y^2 \alpha_2^{1/3}}{a\sqrt{\pi}} >> 1, \quad t >> \frac{s}{c}, \quad t >> t_{SF} \tag{11}$$

where

$$\alpha_1 = \frac{\sqrt{a\sqrt{\pi}\, s}}{4M}, \quad \alpha_2 = \frac{a\sqrt{\pi} s}{4Mk_y}. \tag{12}$$

Thus the asymptotic expressions are valid only for the limited parameter ranges satisfying (10) or (11). Initial conditions are also limited. Therefore a simulation program is needed to study RWBBU more minutely and generally.

RWBBU SIMULATION

A simulation program has been developed to study the RWBBU behaviours and to evaluate effects of the RWBBU on ERLs. Features of this program are as follows:

- Long-range transverse resistive-wall wake
- Lowest mode (dipole mode)
- Rigid and point-like bunches
- 1-D tracking
- Single pass
- Combination of round pipes with/without external focusing or defocusing
- Basic time increment is the bunch separation τ_B divided by an integer N_D (division number)

In order to check the simulation program, simulations are compared with analytic solutions for some special cases. The first is no wake case with uniform external focusing. In this case, the transverse position along the longitudinal location s is just sine-like for all the bunches. Figure 1 shows an example with k_y=3 m^{-1}. The position displacement is normalized by the initial offset y_{00}. The simulation result for N_D=10 is consistent with the exact solution. It should be noted that the division number must be carefully selected for strong focusing, because an insufficient division number leads to an incorrect result as shown for N_D=1 in the figure. The second is non-zero wake case without external focusing for a small bunch number. In this case, Eq. (5) can be analytically solved and the exact solutions are given by

$$y_2(s)/y_{00} = 1 + \frac{1}{2} a s^2 \tag{13}$$

and

$$y_3(s)/y_{00} = 1 + \frac{1}{2}\left(1 + \frac{1}{\sqrt{2}}\right) a s^2 + \frac{1}{24} a^2 s^4 \tag{14}$$

for the second and third bunches (M=2 and 3), respectively. As shown in Fig. 2, the simulation results are in good agreement with the analytic solutions.

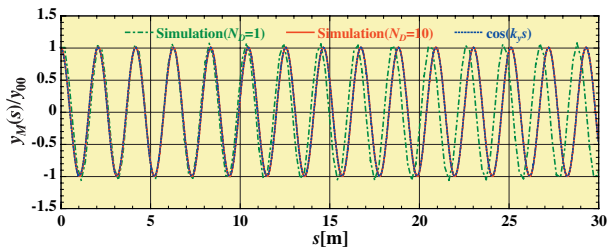

Figure 1: Simulation results (N_D=1,10) and analytic solution cos($k_y s$) for no wake case with external focusing k_y=3 m^{-1}.

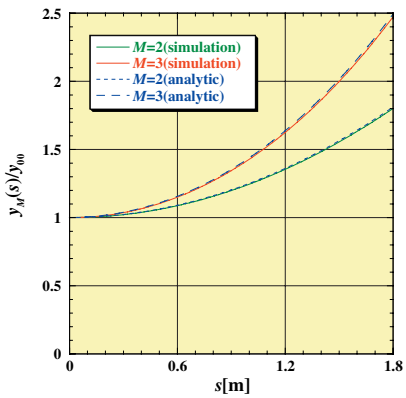

Figure 2: Simulation results and analytic solutions for the second and third bunches (M=2 and 3) in non-zero wake case (a=0.5 m^{-1}) without external focusing.

Next simulations are compared with the asymptotic expressions. Figures 3 and 4 show examples of NF and SF cases. Parameter values were properly chosen for each case so that they should almost satisfy the condition (10) or (11). The blue broken lines indicate the asymptotic expressions and the red solid lines the simulation results. The simulation results are also in agreement with the asymptotic solutions. From these comparisons, it is concluded that the simulation program works well.

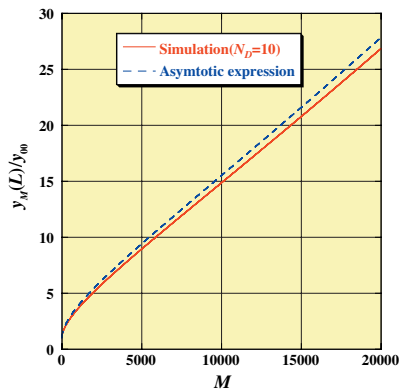

Figure 3: Simulation result (N_D=10) and asymptotic expression for no focusing case (a=2.62x10^{-5} m^{-1}, L=50 m).

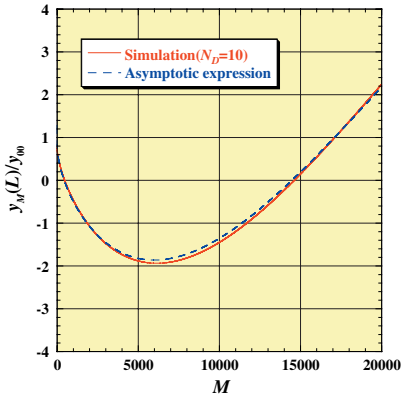

Figure 4: Simulation result (N_D=10) and asymptotic expression for strong focusing case (a=2.62x10^{-3} m^{-1}, k_y=3 m^{-1}, L=10 m).

SIMULATION OF THE TEST ERL

The simulation program was applied to the test ERL in Japan, which is being designed [3]. Figure 5 shows layout of the test ERL. Simulation conditions are as follows:

- Beam energy E=60 MeV, average beam current I_B=100 mA for uniform bunch filling, and bunch separation τ_B=0.769 ns (RF frequency f_{RF} = 1.3 GHz).
- All the vacuum ducts are assumed to be Al pipes with b=25 mm and σ_c=3.5x10^7 Ω^{-1} m^{-1}.
- The simulation start and end points are the exit and entrance of the superconducting cavity section as shown in Fig. 5 and the total path length L is 56.44 m.
- All the bunches have the same initial position offset y_{00} at the simulation start point.
- 1-D tracking in the vertical direction for $t \leq 77$ μs ($M \leq 100000$).
- Focusing and defocusing of 37 quadrupole (Q) magnets in the beam path are considered.
- Sextupole magnet fields, magnet and duct alignment errors, orbit correction by correctors are not considered.
- When the insertion device is considered, its vacuum duct is assumed to be a stainless-steel (SS) pipe with a radius of 10 mm, a conductivity of 1.4x10^6 Ω^{-1} m^{-1} and a length of 10 m.

First a situation with all the Q-magnets off and without the ID is considered for simulation. In this situation the test ERL just equals the Al pipe with a constant radius of 25 mm and a total length of 56.44 m and without external focusing and defocusing. Figure 6 shows position displacement due to resistive-wall wake at the simulation end point (s=L) normalized by the initial position offset y_{00} as function of time t or bunch number M. The normalized position displacement does not depend on the value of y_{00}. The position displacement obtained from the simulation is proportional to $t^{1/2}$ and increases up to 3% of the initial position offset at 77 μs. The asymptotic expression of NF case indicated by the blue broken line in Fig. 6 monotonically decreases with the time and it is not in agreement with the simulation result. For the parameter range, the asymptotic expression is invalid and the simulation is essential for obtaining correct results.

Figures 7 (a) and (b) show orbit distortions y_M(s)-y_1(s) due to the RW wake along the beam pipe with all the Q-magnets off and on, together with initial orbits y_1(s). These initial orbits and orbit distortions are also normalized by the initial position offset y_{00} in the figures. Since every bunch except the first bunch is continuously kicked by the RW wake in the same direction, the orbit distortion monotonically increases with the longitudinal distance s in Fig. 7(a). On the other hand, in Fig. 7(b), the orbit distortion is oscillatory along the beam pipe because the initial orbit is also oscillatory around the pipe center due to the Q-magnet focusing. As a result, the maximum orbit distortion is reduced to 1% of the initial position offset from 3%. Orbit correction is expected to be effective for suppressing the growth of the resistive-wall BBU, though pipe alignment error may still be left even after perfect COD correction. Figures 8 (a) and (b) show conductivity and current dependencies of the RWBBU with all Q-magnets on. In Fig. 8(a), position displacements at the exit for two cases of SS and Al pipes and their ratio are shown as a function of time. The ratio is almost constant and equals the square root of the ratio between electric conductivities of Al and SS. In Fig. 8(b), position displacements for average currents of 100mA and 10mA and their ratio are shown. The ratio is also constant and equals the ratio of the average currents. These results suggest that position displacement due to the RW wake is simply proportional to the wake strength a within the simulated bunch number or time.

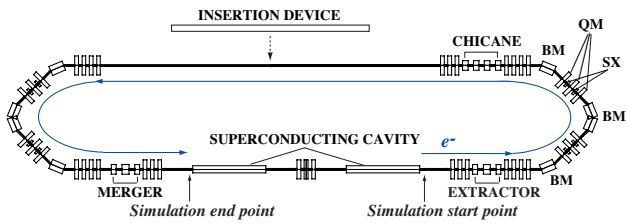

Figure 5: Layout of the test ERL in Japan

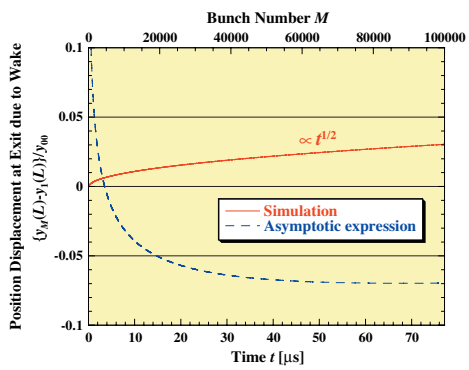

Figure 6: Position displacement at exit due to RW wake with all the Q-magnet off as a function of time and bunch number.

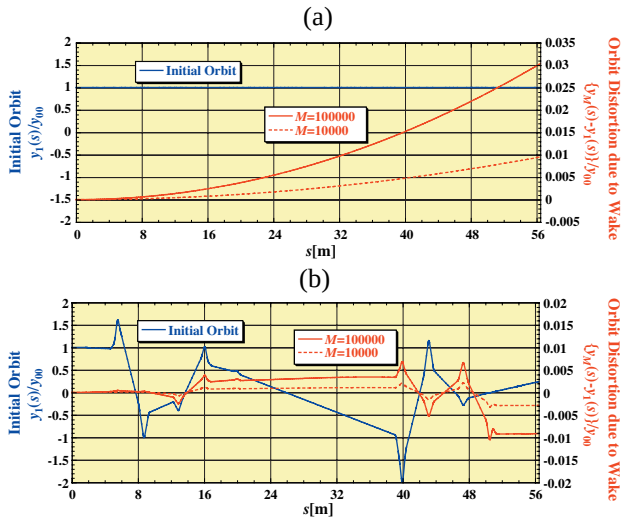

Figure 7: Initial orbits and orbit distortions due to the RW wake for M = 10000 and 100000 with all Q-magnets (a) off and (b) on in the test ERL. The bunch numbers M = 10000 and 100000 correspond to times t = 7.7 and 77 μs.

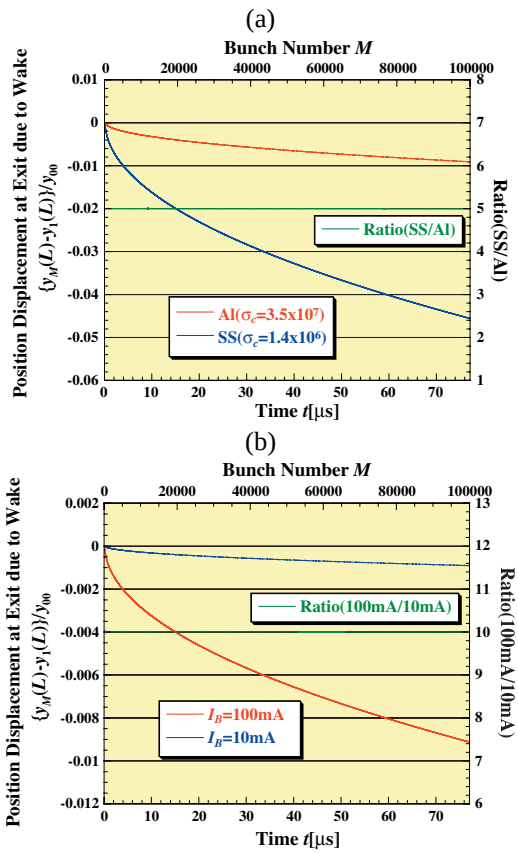

Figure 8: Position displacements at exit due to RW wake (a) for electric conductivities of pipes □c = 1.4x106 □-1 m-1 (SS: stainless steel) and 3.5x107 □-1 m-1 (Al: aluminum) and (b) for the average currents IB = 100 mA and 10 mA with all the Q-magnet on as a function of time. Their ratios are also shown.

Figures 9 (a) and (b) show the effects of a small-gap ID duct and the ID focusing respectively. As shown in Fig. 9(a), simulated orbit distortion due to the RW wake significantly increases downstream of the ID section because of strong resistive-wall wake due to the small-gap ID duct. On the other hand, in Fig. 9(b), the orbit distortion is well reduced because the initial orbit oscillates around the pipe center due to ID focusing (k_y=1 m^{-1}) in the ID section. However the ID focusing strength is changeable in user operation and cannot always be effective for suppression of the RWBBU. A copper-coated SS duct can be effective for reducing the wake strength in the ID section [4].

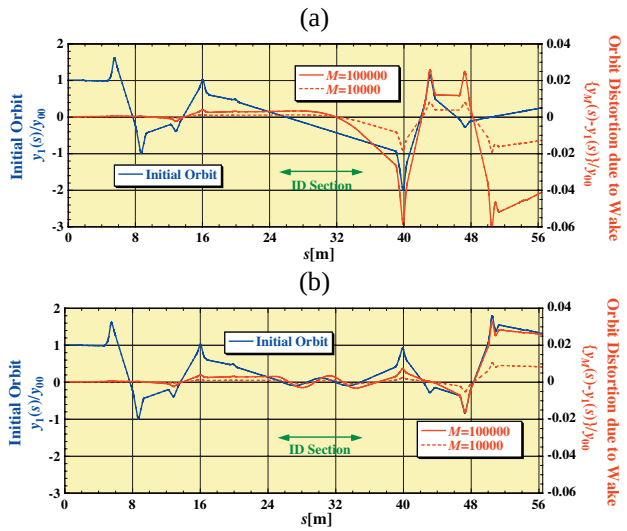

Figure 9: Initial orbits and orbit distortions due to the RW wake for M = 10000 and 100000 (t = 7.7 and 77 μs) with ID focusing strength (a) k_y = 0 m^{-1} and (b) k_y = 1 m^{-1} in a small-gap ID pipe at ID section.

DISCUSSIONS

Parameter Dependencies

In the previous section, the simulation results suggested that the position displacement due to the RWBBU is proportional to $t^{1/2}$ and a. Here the RWBBU behavior is checked with an analytic method. The basic equations of the RWBBU for the initial (M=1) and M-th ($M \geq 2$) bunches are given by

$$y_1''(s) + K_y(s) y_1(s) = 0 \tag{15}$$

$$y_M''(s) + K_y(s) y_M(s) = \sum_{N=1}^{M-1} \frac{a(s)}{\sqrt{M-N}} y_N(s) \quad (M \geq 2) \tag{16}$$

Eq. (16) is identical with Eq. (5) except that uniform focusing strength k_y^2 and wake strength a in Eq. (5) are extended to non-uniform focusing or defocusing strength K_y(s) and wake strength a(s). From these two equations, the following equation is obtained:

$$\xi_M''(s) + K_y(s) \xi_M(s) = \sum_{N=1}^{M-1} \frac{a(s)}{\sqrt{M-N}} \frac{y_N(s)}{y_{00}} \tag{17}$$

where

$$\xi_M(s) \equiv \frac{y_M(s) - y_1(s)}{y_{00}}. \quad (18)$$

$\xi_M(s)$ is the position displacement of the M-th bunch from the initial bunch position normalized by the initial position offset y_{00} and it is caused by the cumulated resistive-wall wake. In the early stage of the RWBBU, this equation is approximately rewritten by

$$\begin{aligned}\xi_M''(s) &\approx \sum_{N=1}^{M-1} \frac{a(s)}{\sqrt{M-N}} \frac{y_1(s)}{y_{00}} \\ &\approx 2\sqrt{M}a(s)\frac{y_1(s)}{y_{00}} \quad (M >> 1)\end{aligned} \quad (19)$$

For $y_M'(0) = y_1'(0)$, $y_M(0) = y_1(0)$, and $a(s) = a$, the following relation is derived from Eq. (19):

$$\begin{aligned}\xi_M(s) &\propto at^{1/2} \\ &\propto \sigma_c^{-1/2} b^{-3} I_B E^{-1} \tau_B^{1/2} t^{1/2}\end{aligned} \quad (20)$$

This relation is consistent with the simulation results in Figs. 6 and 8. In addition, dependencies of the RWBBU on other parameters such as the beam energy, the pipe radius and the bunch separation are foreseen.

Validity of Wakefunction

The validity of the simulation results depends on that of Eq. (1). From the condition of (2), one can estimate the distance z where the wakefunction of Eq. (1) is valid. When all the vacuum ducts of the test ERL are Al pipes with a radius b = 25 mm and an electrical conductivity σ_c = 3.5x10^7 Ω^{-1} m^{-1}, the valid distance range is given by

$$3.62 \times 10^{-5} << z[\mathrm{m}] << 8.24 \times 10^{6} \ . \quad (21)$$

The above distance range is easily converted to the valid time range as

$$1.21 \times 10^{-13} << t[\mathrm{sec}] << 2.75 \times 10^{-2} \ . \quad (22)$$

The upper time limit for the validity of Eq. (1) is 27.5 ms, which corresponds to M=3.575x10^8 and is 3575 times larger than the maximum simulation time, 77 μs. Similarly the valid time ranges for the stainless steel (SS) pipe case (σ_c = 1.4x10^6 Ω^{-1} m^{-1}) are given by

$$3.53 \times 10^{-13} << t[\mathrm{sec}] << 1.10 \times 10^{-3} \quad (b = 25\ \mathrm{mm}) \quad (23)$$

and

$$1.92 \times 10^{-13} << t[\mathrm{sec}] << 1.76 \times 10^{-4} \quad (b = 10\ \mathrm{mm}). \quad (24)$$

The upper time limits for the SS pipe case are 1.1 ms and 176 μs for b=25 mm and b=10 mm. They are still larger than the maximum simulation time and Eq. (1) is valid for both cases. Therefore the parameter values used for the simulations almost satisfy the condition of (2).

Next effects of the pipe thickness are considered. Eq. (1) is derived under the assumption that the pipe thickness is infinite. However such an assumption is not always appropriate. Here the upper time limit is roughly estimated as the inverse of the frequency at which the skin depth is equal to the pipe thickness d. The upper time limit t_{ul} is given by

$$t_{ul} \cong \pi \mu_0 \sigma_c d^2, \quad (25)$$

where μ_0 is the permeability of vacuum. For the Al pipe case with d = 5 mm, the upper time limit is 3.45 ms and larger than the maximum simulation time. On the other hand, for the SS pipe case with d = 2 mm, the upper time limit is 22 μs and smaller than the maximum simulation time of 77 μs. In this case, the wakefunction of Eq. (1) may be somewhat modified. If the simulation time is much increased, even for the Al pipe case, the wakefunction should be modified. The effects of the pipe thickness as well as the pipe conductivity and radius on the wakefunction should be further investigated to understand the RWBBU behaviors at longer times.

SUMMARY AND CONCLUSION

A simulation program of the RWBBU has been developed because the asymptotic expressions are valid only in limited parameter ranges and initial conditions. The simulation program is useful for studying the transverse RWBBU more minutely and generally. The simulation program was applied to the test ERL in Japan. In the simulations, the maximum position displacements with all the Q-magnets off and on are about 3% and 1% of the initial position offset at 77 μs. The Q-magnet focusing contributes to slowing the RWBBU growth and orbit correction is also expected to be effective. A small-gap ID duct significantly increases the orbit distortion, and the ID focusing well suppresses the RWBBU growth, though it is changeable. The RWBBU should be further studied with simulations and the simulation program should also be developed to introduce a new definition of the wakefunction for wider time range, pipe alignment errors, orbit correction due to correctors, non-linear field elements such as sextupole magnets, copper-coating effects on the ID duct wake and so on. Furthermore simulation results should be compared experimentally and quantitatively with operational data of the planned test ERL and/or the existing ERLs to confirm the validity of the simulations. Finally schemes of overcoming the RWBBU must be surveyed and studied, if necessary.

REFERENCES

[1] See, for example, J. M. Filhol et al., "Overview of the Status of the Soleil Project", EPAC'06, Edinburgh, July 2004, p. 249; J. L. Revol and R. Nagaoka, "Observation, modelling and cure of transverse instabilities at the ESRF", PAC'01, Chicago, June 2001, p. 1930.

[2] J. M. Wang and J. Wu, "Cumulative beam breakup due to resistive-wall wake", PRST-AB 7 034402(2004).

[3] K. Harada et al., "Lattice and Optics Designs of the Test ERL in Japan", these proceedings.

[4] N. Nakamura et al., "Reduction in Resistive-Wall Impedance of Insertion-Device Vacuum Chamber by Copper Coating", EPAC'98, Stockholm, August 1998, p984; H. Sakai et al., "Development of Copper Coated Chamber for Third Generation Light Sources", PAC'05, Knoxville, May 2005, p2633